The Hobby-Eberly Telescope Dark Energy Experiment

Gary J. Hill, Karl Gebhardt, Eiichiro Komatsu, Phillip J. MacQueen

McDonald Observatory & Dept. of Astronomy, University of Texas at Austin, 1 University Station, Austin, TX 78712

Abstract. We describe a project (HETDEX) to measure the evolution of dark energy out to z∼4 with high precision. The galaxy power spectrum contains the baryonic oscillations seen in the CMB, and these features remain in the linear regime at high redshift. The separation of these peaks in the power spectrum is a standard ruler imprinted on both the angular and redshift space distribution of galaxies, providing direct constraints on the local Hubble constant H(z) and the angular diameter distance $D_A(z)$, both of which are related to the dark energy equation of state parameter w(z).

We propose the use of Ly-α emitting galaxies as the tracer of the power spectrum, and describe the **V**isible **I**FU **R**eplicable **U**ltra-cheap **S**pectrograph (**VIRUS**), capable of undertaking such a survey. VIRUS will be a very wide field integral field spectrograph of a new replicated design, consisting of more than a hundred individual spectrograph units. The VIRUS instrument mounted on a new wide field corrector on the Hobby-Eberly Telescope (HET) will allow 1 million Ly-α emitting galaxies to be mapped over $1.8 < z < 3.8$ in 200 square degrees of sky, a volume 10 times that of the Sloan Digital Sky Survey (SDSS) in 100 nights of operation. This survey of large scale structure is sufficient to measure the power spectrum to 2-3% accuracy and constrain the positions of the baryonic acoustical peaks on the matter spectrum to $\leq 1\%$. This in turn provides sufficient accuracy on H(z) and $D_A(z)$ to challenge the level of dark energy constraint expected from the SNAP satellite at a fraction of the cost, while providing unique constraints at z>2. The baryonic acoustical peaks method is largely free of systematic biases and provides an independent test of results found by other methods.

1. INTRODUCTION - MEASURING DARK ENERGY

Almost nothing is known of the properties of Dark Energy (DE) beyond its existence. Progress in understanding its physical nature will require precision measurements of the expansion history of the Universe at the level of a few % or better over the redshift range $0 < z < 4$. Such constraints can come from observations of Type Ia supernovae (SNe) (e.g. [1], [2]), large scale surveys of weak lensing (e.g. [3]), surveys of galaxy clusters (e.g. [4]), and observations of the baryonic acoustical oscillations [5] imprinted in the power spectrum of galaxies (e.g. [6],[7], [8]). In order to make progress towards the goal of measuring the expansion history to a few %, very significant surveys involving new facilities are required, and several of these projects are described elsewhere in these proceedings.

The equation of state of DE is expressed as the parameter w(z) [9], [10], the ratio of pressure to density. If DE is described by a cosmological constant, then w(z)=-1, but many forms of w(z) have been proposed such as quintessence [11] which result in dynamically evolving DE that will have a measurable affect on the expansion history. Figure 1 shows several parameterizations of w(z) and the affect they have on the Hubble constant and angular diameter distance as a function of redshift. The obvious constraints on w(z) come from measurement of the local Hubble constant, H(z), and the angular diameter distance $D_A(z)$. SN surveys measure $D_A(z)$ using the SNe as standard candles. However, H(z) is significantly more powerful for constraining w(z) since it is related through one integral, as opposed to $D_A(z)$ which is a double integral (see equations (2) and (3)). The galaxy power spectrum analysis of the baryonic acoustical peaks has the advantage that it measures both H(z) and $D_A(z)$. Another advantage is that it provides high accuracy and is free of systematic biases.

Current constraints from the luminosity distance of type Ia SNe are sufficient to constrain the value of the DE equation of state to about 15% *if* it is assumed to be constant with redshift [2]. Relaxation of this prior removes most of the constraint, allowing a wide range of possible evolution of the DE equation of state (e.g. [14]). Constraints involving SNe are now approaching the level where systematic uncertainties begin to dominate over random errors [13]. The current generation of experiments (ESSENCE (`http://www.ctio.noao.edu/~wsne/`), CFHT SNLS [15], and HST observations [2]) will reach the systematics dominated regime, and improved constraints will require the few

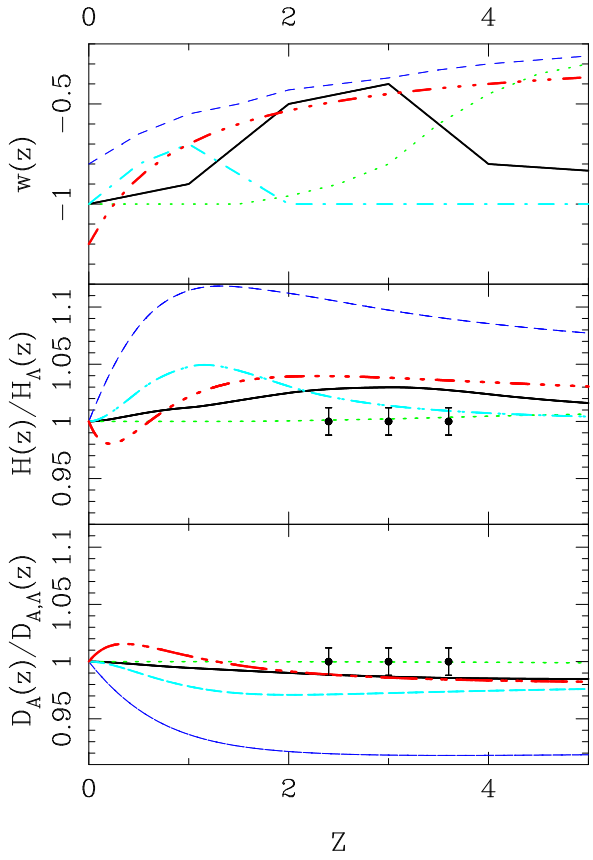

FIGURE 1. Example models of DE evolution. The top panel shows w(z), while the middle panel shows H(z) and the bottom panel shows $D_A(z)$ for the various models. Each model has the same line style in each panel. H(z) and $D_A(z)$ are shown relative to their values for ΛCDM with a cosmological constant. The solid and dash-dot line models are arbitrary, designed to illustrate sensitivities, while the dashed and dotted lines are the SUGRA and 2EXP models taken from [12]. The remaining (dash-dot-dot-dot) curve represents a model that would not be excluded by an improvement of a factor of 10 in the amount of SN data available [13]. 1-σ error bars are shown for the expected sensitivity of the survey described in this paper. The expected accuracy of VIRUS is 1.2% in three redshift bins, both for H(z) and $D_A(z)$. This accuracy is sufficient to distinguish all models compared to the cosmological constant, except for the 2EXP model. Clearly, significant discrimination exists in such a survey to possible evolution of w(z). Note the different behaviour of H(z) and $D_A(z)$.

percent precision offered by SNAP [16]. Constraints obtained by combining the power spectrum of Ly-α absorbers with CMB and SN measurements, provide 20-25% constraints on w(z), for various simplistic parameterizations of w(z), to z=1.4 [17].

2. BARYONIC ACOUSTICAL OSCILLATIONS IN THE GALAXY POWER SPECTRUM

We focus here on constraints that can be obtained on the DE equation of state using the scale size of the baryonic oscillations imprinted on the large-scale structure (LSS) of galaxies. Surveys to provide such constraints have been described by [6], [7], [12], [18], [8], [19], among others. The baryonic acoustical peaks seen in the cosmic microwave background (CMB, e.g. [5]), are imprinted on the matter power spectrum at recombination [20]. The scale size is a standard ruler that can be calculated based on measurements of the CMB anisotropy, and the scale is remarkably robust against systematics [21]

Redshift surveys of LSS can detect the acoustical peaks in the power spectrum of galaxies. The scale size of these peaks will then constrain the local Hubble constant H(z) and the angular diameter distance $D_A(z)$ to that redshift.

These quantities provide a particularly appealing combination since w(z) is related to the first derivative of H(z), (equation (2)) but to the second derivative of angular diameter distance (equation (3)). Given sufficient precision of the measurement at (say) z=3, sensitivity exists to the value of w(z) both at that redshift and its evolution at lower redshifts (see Figure 1).

In contrast to most other methods, which are effective at z$\sim$1.5 and below, constraints from the baryonic oscillations only become tractable at z>1, due to the gravitational evolution of LSS that wipes out the peaks on progressively larger scales. The transition to the linear regime, where the peaks are preserved, at z=1 occurs at wave numbers k<0.2 Mpc^{-1}, with only two peaks linear, but at z>2 the transition moves rapidly to k>0.35 Mpc^{-1} where five peaks are in the linear regime (e.g. [7], [8]). Of course at these redshifts the DE is sub-dominant to (dark) matter, so direct constraints require high precision and, in particular, tight knowledge about Ω_m. Observations of the baryonic oscillations at high redshift would provide the most direct and precise measurement of Ω_m, and hence improve the constraints from other methods applied at lower redshift by e.g. SNAP [12].

A determination of the power spectrum to 2-3% per δk=0.01 Mpc^{-1} bin is sufficient to constrain the separation Δk of the baryonic peaks to <1%, depending on the redshift of the observation (Figure 2, and see [7] and [8]). The most efficient survey balances the need for area (in order to sample the largest scales adequately) and for number statistics (to reduce the Poisson error of the measurement on the smaller scales). The optimum surface density of tracers decreases as the square of the bias of those tracers, and is about 1 object per square arcminute at z=3 if the bias b=3 [7], [8]. Figure 2 shows the error on the power spectrum for a 200 square degree survey of galaxies with Δz=1 and b=3.5, sampled at n=0.5 and 1.0 objects per square arcminute. The largest scale (low k) results are less affected by the number of tracers than are the results on small scales.

The measurement of the galaxy power spectrum yields a fit to the value of Δk in both the transverse (angular) and radial (redshift) directions. The fit for the aforementioned 200 square degree, z$\sim$3 survey is shown in Figure 3. These are independent measurements with different dependencies on w(z). The equations governing the relationship between the measurements and the equation of state of the DE are simple, for a closed universe:

$$r_s = (1+z)D_A(z)\Delta\theta = c\frac{\Delta z}{H(z)} \tag{1}$$

where r_s is the comoving scale of the sound horizon as measured from the CMB, $\Delta\theta$ is the angular separation of the acoustic peaks in the power spectrum, and Δz is their separation in redshift space. The local Hubble constant H(z) and the angular diameter distance D_A(z) are given by:

$$H(z) = h\sqrt{\Omega_m(1+z)^3 + \Omega_X exp[3\int\frac{1+w(z)}{1+z}dz]} \tag{2}$$

$$D_A(z) = \frac{c}{1+z}\int\frac{dz}{H(z)} \tag{3}$$

Each method of determining the scale size evolution of the Universe has its own set of systematic uncertainties, but the Baryonic oscillation method is relatively free of systematics. The separation of the peaks, set by the sound horizon at recombination, is known to 1.3% [5]. The precision of the measurement depends on the accuracy to which $\Omega_m h^2$ is known. The precision should improve to 0.9% with four years of WMAP data, and will improve further to 0.3% with the Planck Satellite [22]. This level is about twice as accurate as that achieved with the above-mentioned z$\sim$3, 200 square degree survey.

Bias, b, [23] is the degree to which a given tracer provides an amplified measure of the cross correlation function of the underlying dark matter fluctuations. Having a tracer with high bias benefits the measurement of the power spectrum, requiring fewer objects by a factor of b^2 [7], [8]. We expect LAEs to have a bias equal to or larger than the underlying dark matter. The dark matter halo bias is larger than unity for masses larger than the non-linear mass (above which, the mass function is exponentially suppressed) [24]. The relation between dark matter halo bias and galaxy bias is rather uncertain. However, the galaxy bias will be larger than the dark matter bias if the number of galaxies per halo mass is greater than the mean number density of galaxies per mean mass density of the universe [8]. This is certainly true for LAEs at high redshift. We expect b$\sim$3.5, similar to that of Lyman break galaxies (LBGs e.g. [25]). While bias varies with galaxy mass, it would require a very contrived variation of bias with wavenumber to shift the positions of the baryonic acoustical peaks in the power spectrum to any appreciable degree. Any monotonic variation of b(k) will not cause systematic errors in the measurement.

Redshift space distortions [26], [27], cause a net inflow into overdense regions and a net outflow from underdense regions. This effect will compress the scale size of the acoustic peaks in redshift space, due to the gravitational

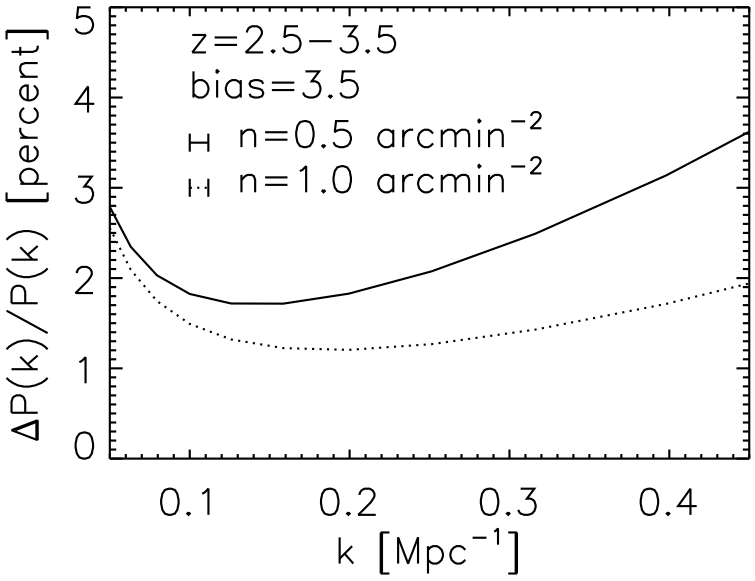

FIGURE 2. Simulation of HETDEX errors on the power spectrum. The error in P(k) as a function of k for a dataset of two 100 square degree fields with Δz=1 at z=3 is shown. Bias of 3.5 is assumed for the tracer galaxies. The resolution in k is 0.01 Mpc^{-1}. The solid curve is for a tracer surface density of 0.5 objects per square arcminute, and the dashed line is for 1.0 objects per square arcminute. The rise at high k is due to Poisson noise, and the upturn at low k is due to the survey volume.

attraction of overdensities canceling part of the Hubble expansion. This affects the linear regime and must be corrected since it directly alters the determination of H(z). The effect depends on Ω_m and the bias [26], and it is possible to model its effect sufficiently via the quadrupole moment of the cross-correlation function, that it will have little affect on the precision of the determination of H(z), as has been done for 2dF, for example [27]. The 'Finger of God' effect caused by random motions within groups is an effect of the small-scale non-linear regime and is not relevant here.

There are two possible tracers of LSS at z$\sim$3. Lyman break galaxies (LBGs) have been suggested as a natural tracer (e.g. [6], [8], [12]), being selected as U-band drop-outs in deep broad-band imaging surveys and having a surface density of about 1 per square arcminute. The candidates could be targeted by a next generation multi-object spectrograph on a 6-8 m class telescope with a very wide field of view [6]. The aperture is needed to reach sufficient S/N ratio to use absorption lines to secure the redshifts in 1 hour exposures. The proposed KAOS instrument [28] is an example.

An alternative tracer is the more numerous Ly-α emitting (LAE) galaxy population. LAEs have the advantage of having strong emission lines, so shorter integrations are possible, and their space density is five times higher than for LBGs (depending on the detection limits). Narrow band imaging surveys (e.g. [29], [30], [31]) find surface densities of LAEs to be between 4 and 5 per square arcminute at a line flux limit of 2x10^{-17} erg/cm^2/s. While long exposures are needed with narrow band filters to detect such objects, they can be detected spectroscopically in a matter of minutes. The width of the narrow band filters and confusion with field galaxies that have a dispersion in color between the line and continuum filters dominate the detection limit, rather than photon statistics.

LAEs are ideal tracers if an integral field unit (IFU) spectrograph with very wide field of view can be constructed for a 6-8 m class telescope. Currently, the largest IFU fields of view are about one square arcminute ([32], [33]), whereas coverage of about 30 square arcminutes would be needed to survey a useful volume in a reasonable amount of time. In the next section we describe how such an instrument can be realized to survey 200 square degrees with Δz=2 in 100 nights of time with the 9.2 m Hobby-Eberly Telescope. This survey would have a total volume of about 6 Gpc^3, or ten times the volume of the main part of the SDSS (`http://www.sdss.org/`), sufficient to achieve the accuracy on the power spectrum illustrated in Figures 2 and 3.

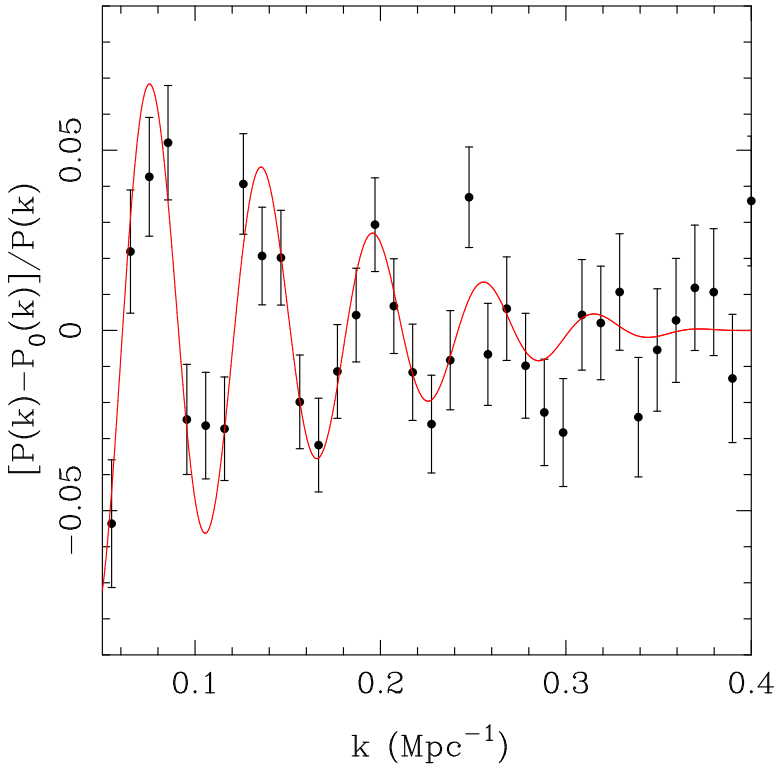

FIGURE 3. Simulation of the fit to the baryonic oscillations in the power spectrum for the n=1 object per square arcminute case using errors indicated in Figure 2. The fit has a single variable of the separation Δk of the peaks, and the error on this quantity is 0.7%. If the range of k is restricted to k<0.2 Mpc^{-1}, the non-linear scale size at z=1.5, then the resulting error on the fit is 1.0%. This comparison illustrates the power of working at the higher redshift, including more linear peaks in the fit. For the full survey of 200 square degrees with Δz=1.9, we can expect error bars on $\Delta\theta$ and Δz (see equation (1)) of 1.2% in three bins of redshift over 2 $<$ z $<$ 4, since the surface density is expected to be approximately constant with redshift, see text.

3. THE HOBBY-EBERLY TELESCOPE AND VIRUS

In astronomy, instruments have typically been of monolithic, one-off, design, where the majority of funds are expended on engineering effort. The next generation of telescopes and wide fields will require a new paradigm in order to limit the cost and complexity of instruments. The concept of industrial replication [34], [35], where of order a hundred or more modular spectrographs combine to form a whole, allows the engineering cost to be amortized over many units, driving down the total cost. Industrial replication offers significant cost-advantages (roughly a factor of two) when compared to a traditional monolithic spectrograph, particularly in the cost of the optics and engineering effort [34]. Here we apply the concept to the 9.2 m Hobby-Eberly Telescope with 132 simple IFU spectrograph modules arrayed in a fixed pattern, projected on the sky, for wide area surveys. The **V**isible **I**FU **R**eplicable **U**ltra-cheap **S**pectrograph (**VIRUS**, [35]) module consists of a fiber-coupled IFU feeding a single, simple spectrograph. The design and construction of each VIRUS module is well within the state of the art, and industrial replication is used to build many copies of the module to be integrated into a single instrument.

The VIRUS design is described in more detail in [35]. Each module covers 28x28 square arcseconds on the sky with a DensePak type [36] fiber IFU. The fibers will be packed in a hexagonal pattern with a fill factor of 1/3. Each fiber has 1 square arcseconds area, and three exposures dithered to fill in the area would then cover 28x28 square arcseconds. The light from the 247 fibers is dispersed over the wavelength range 340 - 570 nm at a resolving power of about 800, covering 1.8 $<$ z $<$ 3.7 for Ly-α emission. The input f/ratio will be about f/3 to minimize focal ratio degradation in the fibers, and the collimator would feed a volume phase holographic grating disperser and a refractive camera with a final speed of about f/1.4. The detector will be a 2kx2k CCD with 13.5 or 15.0 μm pixels. The design and manufacture of VIRUS is well within the state of the art. The challenge comes from replicating the spectrograph modules 132-fold (VIRUS-132) to cover the required 30 square arcminutes per observation. This requires

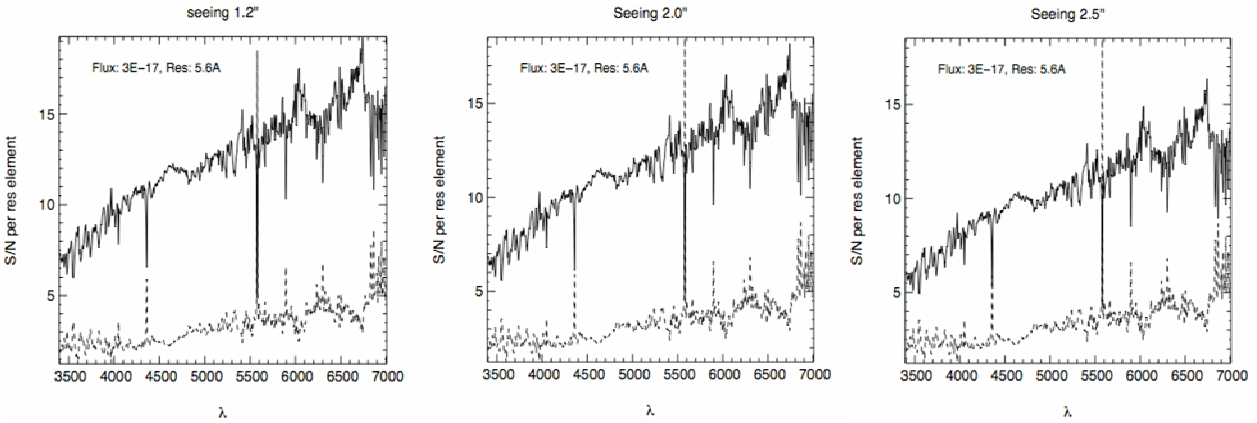

FIGURE 4. Sensitivity of VIRUS under various seeing conditions for six 200 second exposures. The position on the sky would be dithered between exposures to fill in the dead space between fibers in the IFUs. Each panel shows the S/N ratio for a fiducial line flux of 3x10^{-17} erg/cm^2/s as the solid line. The dashed line shows the ratio of noise from sky photons to read-noise from the CCD (assumed to be 2.7 electrons). The observations are sky noise dominated at all wavelengths. The three panels show that seeing from around the median up to even 2.5 arcseconds has little effect on the sensitivity. This is because the sky signal, which dominates the noise, comes from 3 fibers with total area of 3 square arcseconds.

engineering for mass production, which is different from techniques applied typically to astronomical instruments. On an 8-m class telescope like HET under typical conditions, this instrument can reach a 5-σ line flux sensitivity of 2 (0.8) x10^{-17} erg/cm^2/s at the blue (red) wavelength limits respectively [35], as shown in Figure 3. This figure shows the effect of seeing on the sensitivity of the observations, for seeing as large as 2.5 arcseconds. The relatively large size of the fibers projected on the sky means that the sensitivity limit is very insensitive to seeing degradation. Note that the median seeing for the site is about 1.0 arcseconds and the HET is delivering about 1.5 arcseconds median images, currently [37]. HET image quality will improve to close to site-limited with the advent of closed-loop control of the tracker.

These sensitivity limits can be compared with a theoretical fit to the density of LAEs detected in narrow band imaging surveys at redshifts from 2 to 5 [38]. Model A of [38] shows that VIRUS with the above sensitivity limits would detect a surface density of LAEs of $\sim$5.5 per square arcminute, per Δz=1, approximately constant with redshift over the $1.8 < z < 3.7$ range of the observation.

The HET has pioneered a design with a fixed spherical primary and a tracker to follow the motions of objects [37]. The design is particularly effective for surveys. The current HET prime focus corrector covers only a 4-arcminute diameter field of view, with poor image quality and considerable vignetting in the outer field. A new corrector is required to feed VIRUS, and is currently being designed with a field diameter in the range of 15 to 20 arcminutes. One design produces unvignetted, excellent image quality over the anticipated science field of view, with additional field for optical closed-loop tracking control of the corrector position relative to the primary mirror. The layout of the 132 IFUs of VIRUS-132 at the focal surface of HET is shown in Figure 5, and Figure 6 shows a possible telescope layout. The fill factor of the IFUs is 1/7, which provides almost the required $\sim$1 per square arcminute surface density of LAEs, while still sampling well below the non-linear scale size at $z < 4$. The central block of fibers covers 3.5 square arcminutes and enables other science projects on extended objects such as galaxies.

Figure 6 shows a possible arrangement of the 132 spectrograph modules on the HET tracker. The main beam of the tracker, which moves back and forth on the top hexagon of the telescope structure, is shown with the carriage that moves up and down the beam. The corrector is moved to remain perpendicular to the primary mirror and in focus, by a hexapod system. The modules of VIRUS would ride on a separate rotation stage on the carriage, so would not load the hexapod system. This arrangement allows short fibers and fits within the central obstruction of the corrector, but does present challenges for weight and cooling of the detectors. A more straight-forward approach would be to array the modules at the top of the tracker beam, using longer fibers ($\sim$10 m). Longer fibers have more absorption in the UV, but the sensitivities shown in Figure 3 were calculated assuming 10 m fiber length, and the science would not be compromised by this approach. Detailed engineering studies will help to choose between these mounting options.

The detector system for VIRUS will be modularized, highly parallel, and specific to the instrument. In order to

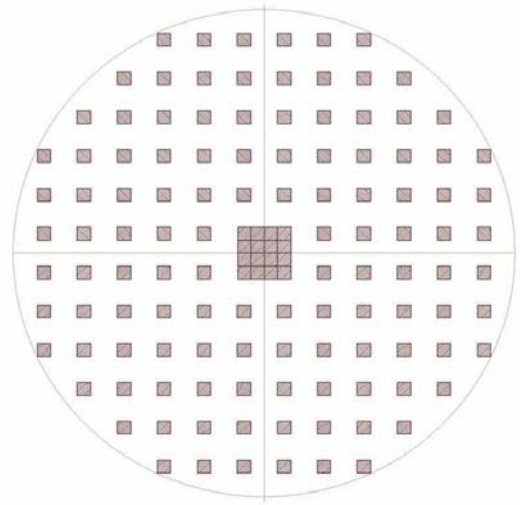

FIGURE 5. Layout of the IFUs for VIRUS-132 on the sky. The diameter of the circle is 16.5 arcminutes, and the effective fill factor of the IFUs is $1/7$. The central block of 16 IFUs would have contiguous coverage of 3.5 square arcminutes, and would enable studies of smaller extended objects. note that the non-linear scale size, below which information is lost in the power spectrum due to gravitational clustering evolution, is equal to three times the separation of the IFUs, so aliasing of this window function will not be an issue. The pointing centers of observations will be randomized to destroy any coherent aliasing of this pattern over the entire survey.

achieve this we will simplify and repackage the McDonald Observatory Version 2 CCD controller so that all the analog electronics are mounted to the detector cryostats, allowing a compact, minimum weight design. Replication and testing techniques used in consumer electronics manufacture will be utilized to cut costs and production time, and to yield the necessary reliability for an electronic system of this size. The Version 2 controller achieves 2.7 electrons read noise with typical detectors at 100 kpixel/second readout rates. The CCDs would be binned by a factor of two in the spatial dimension, so the readout time would be about 20 seconds. The readout would be fully parallel, allowing very low overhead. The data-rate for VIRUS-132 will be $\sim$0.5 GByte per exposure, and the full survey is expected to generate $\sim$10 TByte of raw data.

The design of the survey is being optimized, but we expect to observe two or three high latitude, high declination fields during the spring. HET has the longest track times ($\sim$ 5 hours on target per night) at $\delta \sim$63 degrees declination. Working close to this declination will allow square fields to be observed without breaks in observing. This approach will maximize the efficiency of the survey. With the above sensitivity and readout times, it should be possible to cover an area $\sim$2 square degrees per night with $\sim 1/7$ fill factor. Each night's data would detect about 11,000 LAEs. In 100 nights, more than 1 million galaxies would be surveyed over a volume of 6 Gpc^3. We estimate that it will be possible to complete the survey in three spring trimesters, utilizing the dark time with good transparency. Even the data from the first trimester of observing will provide interesting limits on w(z)

The development of VIRUS will first involve the design and construction of a prototype module. This effort is underway, with the aim of testing the performance in summer 2005. At that point costing of the replication of the full VIRUS will be possible. Fabrication of the full instrument is estimated to require three years, and the survey will take a further 2.5 years to complete. With funding, results could be available in 2010.

4. DISCUSSION AND SUMMARY

We have shown how the very large scale HETDEX galaxy redshift survey using LAEs as tracers can provide constraints on the evolution of the dark energy equation of state parameter w(z) comparable to those from SNAP. The constraints come from detecting the baryonic acoustic peaks in the galaxy power spectrum. The key attributes of this survey are that it would constrain both H(z) and D_A(z) to $\sim$1.2% at three redshifts between $1.8 < z < 3.7$, by observing the wavelength range 340-570 nm simultaneously. H(z) is related to the integral of w(z) while D_A(z) is related to the integral of H(z), and so they have different behaviour under a varying w(z). As a result, they can distinguish between a

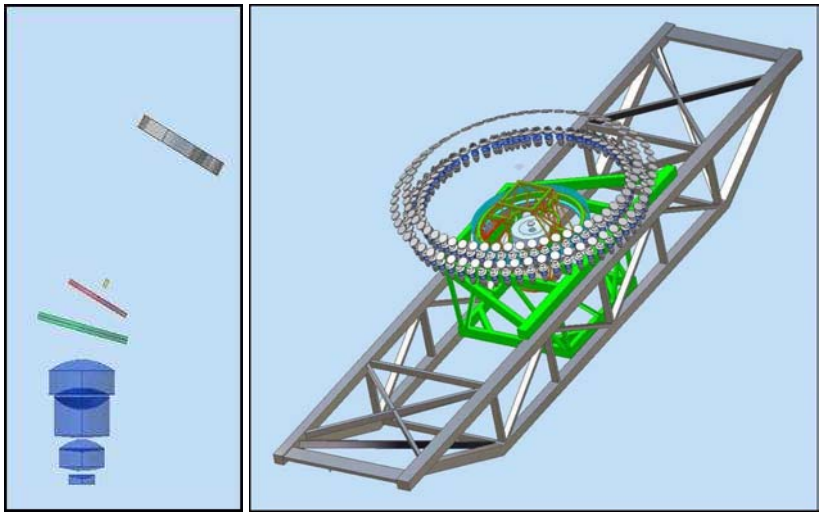

FIGURE 6. One possible layout of VIRUS-132 on the HET. The figure shows a rendition of where VIRUS might be located on the HET. The left panel is a solid model of a VIRUS unit spectrograph with reflective collimator and refractive camera. The total height is about 0.6 m. The right panel shows the main tracker beam of the HET, with the VIRUS modules arrayed around the tracker carriage. In this case the fibers would loop from the focal surface to each of the spectrographs, and could be as short as 2-3 m. The other alternative is to use $\sim$10 m fibers and to site VIRUS at the top of the tracker beam. That location would be most straight-forward from the point of view of weight and cooling the detectors. The loss of throughput in the blue due to the fiber length would not be enough to compromise the experiment.

constant w(z) under ΛCDM and a varying w(z) at the percent level. This sensitivity rivals or exceeds that predicted for the SNAP satellite, and the extended redshift coverage of the HETDEX survey provides an extra lever-arm to search for evolution at $z>1.5$ that SNAP and other experiments will not be able to probe.

Comparable constraints would be obtained from a survey of Lyman break galaxies (LBGs) at $z\sim3$, if a similar volume (10 times that of the SDSS) were probed [7], [8]. LBGs have the optimum surface density of $\sim$1 per square arcminute. Detection of LBGs is restricted to $z>3$ by the need to use U-band photometry to select samples. As a result, the depth of such a survey would be restricted to $\Delta z\sim1$, and 400 square degrees would need to be surveyed. Such a survey would be possible with the proposed KAOS instrument [28], with hour exposures to secure redshifts.

Surveys of LSS to constrain w(z) at lower redshift are feasible at redshifts above $z\sim1$. Below this redshift the gravitational clustering evolution begins to affect the second peak in the oscillation spectrum. Constraints at this lower redshift require more area and must target luminous red galaxies selected in multi-color imaging surveys. Hα emission or continuum absorption features can be used to measure redshifts. The former requires a wide field multi-object near infrared spectrograph such as FMOS on the Subaru Telescope (`http://www.std.rl.ac.uk/fmos/`). The significant drawback of a survey at $z\sim1.0$-1.5 is the reduced sensitivity to evolution of w(z), when compared to the survey described here at $z\sim3$.

Photometric surveys using the angular power spectrum to probe just $D_A(z)$, with photometric redshifts to prevent smearing fail to achieve the level of precision required for significant constraints (e.g. [8], [39]), and the loss of the measurement of H(z) removes a key advantage of the Baryonic peaks to constrain the scale size evolution of the Universe in a different way.

In summary, HETDEX with the proposed VIRUS instrument will provide constraints on w(z) comparable to those expected from SNAP and other forthcoming experiments at a fraction of the cost, and promises to deliver those constraints on a shorter timeframe. In addition, the prospect of probing a higher redshift regime than is possible with SNe, weak lensing or galaxy cluster surveys, opens up the possibility of constraining possible evolution of w(z) in unique ways. Finally, it is important to attack the problem of dark energy from a variety of angles, and the baryonic peaks provide a complementary and independent test, with very few systematic biases.

ACKNOWLEDGMENTS

We wish to acknowledge interesting and useful discussions with C. Blake, D. Eisenstein, H.-J. Seo, S. Rawlings, P. Shapiro, E.L. Robinson, C. Wheeler, J. Kormendy, N. Evans, and D. Dicus. Important contributions to this work have been made by F. Cobos, C. Tejada, N. Drory, P. Palunas, R. Bender, U. Hopp, P. Schuecker, C. Goessl, and G. Wesley. We thank the McDonald Observatory of the University of Texas at Austin for support of this project. GJH thanks the staff of the Instituto de Astronomia, UNAM, Mexico for their hospitality during the development of the optical design for VIRUS.

REFERENCES

1. Perlmutter, S., Aldering, G., Goldhaber, G., Knop, R. A., Nugent, P., Castro, P. G., Deustua, S., Fabbro, S., Goobar, A., Groom, D. E., Hook, I. M., Kim, A. G., Kim, M. Y., Lee, J. C., Nunes, N. J., Pain, R., Pennypacker, C. R., Quimby, R., Lidman, C., Ellis, R. S., Irwin, M., McMahon, R. G., Ruiz-Lapuente, P., Walton, N., Schaefer, B., Boyle, B. J., Filippenko, A. V., Matheson, T., Fruchter, A. S., Panagia, N., Newberg, H. J. M., Couch, W. J., and The Supernova Cosmology Project, ApJ, **517**, 565–586 (1999).
2. Riess, A. G., Strolger, L., Tonry, J., Casertano, S., Ferguson, H. C., Mobasher, B., Challis, P., Filippenko, A. V., Jha, S., Li, W., Chornock, R., Kirshner, R. P., Leibundgut, B., Dickinson, M., Livio, M., Giavalisco, M., Steidel, C. C., Benítez, T., and Tsvetanov, Z., ApJ, **607**, 665–687 (2004).
3. Hu, W., and Jain, B., Phys. Rev. D, **70**, 043009–+ (2004).
4. Wang, S., Khoury, J., Haiman, Z., and May, M., *astro-ph/0406331* (2004).
5. Spergel, D. N., Verde, L., Peiris, H. V., Komatsu, E., Nolta, M. R., Bennett, C. L., Halpern, M., Hinshaw, G., Jarosik, N., Kogut, A., Limon, M., Meyer, S. S., Page, L., Tucker, G. S., Weiland, J. L., Wollack, E., and Wright, E. L., ApJS, **148**, 175–194 (2003).
6. Eisenstein, D., "Large-Scale Structure Future Surveys," in *ASP Conf. Ser. 280: Next Generation Wide-Field Multi-Object Spectroscopy*, 2002, pp. 35–+.
7. Blake, C., and Glazebrook, K., ApJ, **594**, 665–673 (2003).
8. Seo, H., and Eisenstein, D. J., ApJ, **598**, 720–740 (2003).
9. Steinhardt, P. J., "Comments on how Forthcoming Progress in Cosmology Might Influence Fundamental Physics," in *Critical Dialogues in Cosmology*, 1997, pp. 407–+.
10. Turner, M. S., and White, M., Phys. Rev. D, **56**, 4439– (1997).
11. Caldwell, R. R., Dave, R., and Steinhardt, P. J., Ap&SS, **261**, 303–310 (1998).
12. Linder, E. V., Phys. Rev. D, **68**, 083504–+ (2003).
13. Linder, E. V., and Miquel, R., *astro-ph/0409411* (2004).
14. Dicus, D. A., and Repko, W. W., *astro-ph/0407094* (2004).
15. Pritchett, C. L., *astro-ph/0406242* (2004).
16. Aldering, G., and SNAP Collaboration, *astro-ph/0405232* (2004).
17. Seljak, U., Makarov, A., McDonald, P., Anderson, S., Bahcall, N., Brinkmann, J., Burles, S., Cen, R., Doi, M., Gunn, J., Ivezic, Z., Kent, S., Lupton, R., Munn, J., Nichol, R., Ostriker, J., Schlegel, D., Tegmark, M., Van den Berk, D., Weinberg, D., and York, D., *astro-ph/0407372* (2004).
18. Hu, W., and Haiman, Z., Phys. Rev. D, **68**, 063004–+ (2003).
19. Matsubara, T., and Szalay, A. S., *Physical Review Letters*, **90**, 021302–+ (2003).
20. Eisenstein, D. J., and Hu, W., ApJ, **496**, 605–+ (1998).
21. Eisenstein, D., and White, M., *astro-ph/0407539* (2004).
22. Bond, J. R., Contaldi, C. R., Lewis, A. M., and Pogosyan, D., *astro-ph/0406195* (2004).
23. Kaiser, N., ApJ, **284**, L9–L12 (1984).
24. Seljak, U., MNRAS, **318**, 203–213 (2000).
25. Steidel, C. C., Adelberger, K. L., Giavalisco, M., Dickinson, M., and Pettini, M., ApJ, **519**, 1–17 (1999).
26. Hamilton, A. J. S., ApJ, **385**, L5–L8 (1992).
27. Hawkins, E., Maddox, S., Cole, S., Lahav, O., Madgwick, D. S., Norberg, P., Peacock, J. A., Baldry, I. K., Baugh, C. M., Bland-Hawthorn, J., Bridges, T., Cannon, R., Colless, M., Collins, C., Couch, W., Dalton, G., De Propris, R., Driver, S. P., Efstathiou, G., Ellis, R. S., Frenk, C. S., Glazebrook, K., Jackson, C., Jones, B., Lewis, I., Lumsden, S., Percival, W., Peterson, B. A., Sutherland, W., and Taylor, K., MNRAS, **346**, 78–96 (2003).
28. Barden, S. C., Boyle, B., and Glazebrook, K., "KAOS: kilo-aperture optical spectrograph," in *Ground-based Instrumentation for Astronomy. Edited by Moorwood, A.F.M and Iye, M. Proceedings of the SPIE, Volume 5492, in press (2004).*, 2004, p. in press.
29. Cowie, L. L., and Hu, E. M., AJ, **115**, 1319–1328 (1998).
30. Kudritzki, R.-P., Méndez, R. H., Feldmeier, J. J., Ciardullo, R., Jacoby, G. H., Freeman, K. C., Arnaboldi, M., Capaccioli, M., Gerhard, O., and Ford, H. C., ApJ, **536**, 19–30 (2000).
31. Steidel, C. C., Adelberger, K. L., Shapley, A. E., Pettini, M., Dickinson, M., and Giavalisco, M., ApJ, **532**, 170–182 (2000).

32. Prieto, E., Le Fevre, O., Saisse, M., Voet, C., and Bonneville, C., "Very wide integral field unit of VIRMOS for the VLT: design and performances," in *Proc. SPIE Vol. 4008, p. 510-521, Optical and IR Telescope Instrumentation and Detectors, Masanori Iye; Alan F. Moorwood; Eds.*, 2000, pp. 510–521.
33. Kelz, A., Roth, M. M., and Becker, T., "Commissioning of the PMAS 3D-spectrograph," in *Instrument Design and Performance for Optical/Infrared Ground-based Telescopes. Edited by Iye, Masanori; Moorwood, Alan F. M. Proceedings of the SPIE, Volume 4841, pp. 1057-1066 (2003).*, 2003, pp. 1057–1066.
34. Hill, G. J., and MacQueen, P. J., "VIRUS: an ultracheap 1000-object IFU spectrograph," in *Survey and Other Telescope Technologies and Discoveries. Edited by Tyson, J. Anthony; Wolff, Sidney. Proceedings of the SPIE, Volume 4836, pp. 306-312 (2002).*, 2002, pp. 306–312.
35. Hill, G. J., MacQueen, P. J., Tejada, C., and Cobos, F., "VIRUS: a massively replicated IFU spectrograph for HET," in *Ground-based Instrumentation for Astronomy. Edited by Moorwood, A.F.M and Iye, M. Proceedings of the SPIE, Volume 5492*,, 2004, p. 251.
36. Barden, S. C., and Wade, R. A., "DensePak and spectral imaging with fiber optics," in *ASP Conf. Ser. 3: Fiber Optics in Astronomy*, 1988, pp. 113–124.
37. Hill, G. J., MacQueen, P. J., Ramsey, L. W., and Shetrone, M. D., "Performance of the Hobby-Eberly Telescope and facility instruments," in *Ground-based Instrumentation for Astronomy. Edited by Moorwood, A.F.M and Iye, M. Proceedings of the SPIE, Volume 5492*,, 2004, p. 94.
38. Le Delliou, M., Lacey, C., Baugh, C., Guiderdoni, B., Bacon, R., Courtois, H., Sousbie, T., and Morris, S. L., *astro-ph/0405304* (2004).
39. Dolney, D., Jain, B., and Takada, M., *astro-ph/0409445* (2004).